Microelectronic Engineering 99 (2012) 50–57

Contents lists available at SciVerse ScienceDirect

Microelectronic Engineering

journal homepage: www.elsevier.com/locate/mee

Influence of illumination intensity and temperature on the electrical characteristics of an Al/p-GaAs/In structure prepared by thermal evaporation

M. Soylu [a], A. A. Al-Ghamdi [b], F. Yakuphanoglu [b,c,*]

[a] Bingol University, Faculty of Sciences and Arts, Department of Physics, Bingol, Turkey
[b] Department of Physics, Faculty of Sciences, King Abdulaziz University, Jeddah, Saudi Arabia
[c] Department of Physics, Faculty of Science, Firat University, Elazig 23169, Turkey

ARTICLE INFO

Article history:
Received 9 November 2010
Received in revised form 17 January 2012
Accepted 5 July 2012
Available online 20 July 2012

Keywords:
Al/p-GaAs barrier diode
Illumination effect
Temperature effect
Electrical properties

ABSTRACT

The temperature and illumination intensity dependence of current–voltage (*I-V*) and capacitance–voltage (*C-V*) characteristics of the Al/p-GaAs barrier diode were investigated. The ideality factor (n) and zero-bias barrier height (Φ_{b0}) were found to be strongly temperature dependent and while Φ_{b0} is decreased, n is increased with decreasing temperature and illumination. The reverse biased *I-V* measurements under various illuminations exhibited a high photosensitivity. The values of R_s obtained from Cheung's method are decreased with increasing illumination intensity. The interface capacitance of the diode is increased with the increase of illumination intensities. The profiles of interface state density (N_{ss}) distribution as a function of (E_{ss}–E_v) were extracted from the forward *I–V* measurements by taking into account the bias dependence of the effective barrier heights (ϕ_e) for device under dark, illumination and temperature conditions. Furthermore, modified Richardson plot has a good linearity over the investigated temperature range. As a result, the electrical characteristics of diode are affected not only in illumination but also in temperature. It is evaluated that the prepared diode can be used as photocapacitance sensor in modern electronic and optoelectronic devices.

© 2012 Elsevier B.V. All rights reserved.

1. Introduction

The metal–semiconductor (MS) structures have an important role in modern electronics, and MS structures are one of the most important solid-state components in microelectronic integrated circuits [1–6]. These applications consist of microwave field effect transistors, radio-frequency detectors, phototransistors, heterojunction bipolar transistors, quantum confinement devices and space solar cell. There are currently a vast number of reports of experimental studies of characteristic parameters such as the barrier height and ideality factor in a great variety of MS contacts [7–10]. The main characteristic parameters of MS contacts can vary as a function of the various factors. Therefore, it is interesting to investigate the effects of the illumination and temperature on the performance of these devices. When Schottky junctions with electronic based semiconductors are illuminated with photons whose energy values are greater than the energy band gap of semiconductor (E_g), electron–hole pairs are produced in the depletion region of the semiconductor, these devices show a photovoltaic effect. Furthermore, organic interfacial metal–semiconductor contacts have been extensively investigated due to their potential use in a variety of organic electronic and optoelectronic devices, such as field effect transistors [11], organic light-emitting diodes (OLEDs) [12], photovoltaic (PV) cells [13–15] and photo detectors [16]. Current–voltage (*I–V*) characteristics of Cu/p-Si device have been investigated under dark and light illumination. The photocurrent is higher than the dark current at the same reverse bias [17]. The energy distribution profile of N_{ss} was determined from the forward bias *I–V* characteristics by taking the bias dependence of the effective barrier height into account. The density of interface states is decreased with the increasing illumination intensity [18]. In recent years, there has been an explosion in the use of capacitive sensing interfaces for human-input controls. From mobile handsets to computers, point-of-service terminals to home electronics and medical devices to industrial controls, capacitive sensing is showing up in applications everywhere [19].

On the other hand, in order to understand the conduction mechanism of the Schottky barrier diodes (SBDs), many attempts have been made. There are various models such as Schottky, Poole–Frenkel and space charge limited-conduction (SCLC) mechanisms to explain charge transport mechanisms in various materials [20]. The electronic properties of semiconductor materials are strongly affected by the presence of carrier trapping centers in forbidden band gap. The space charge limited-current technique is used to explain electrical properties of semiconductor and insulator materials, and in this model, current shows a power-law dependence on applied voltage, $I \propto V^m$ [21]. But, the analysis of the current–voltage (*I–V*) characteristics of Schottky barrier diodes

* Corresponding author at: Physics Department, Faculty of Science, Firat University, Elazig, Turkey. Tel.: +90 424 237 00 00x3621; fax: +90 424 233 00 62.
E-mail addresses: fyhanoglu@firat.edu.tr, fyhan@hotmail.com (F. Yakuphanoglu).

0167-9317/$ - see front matter © 2012 Elsevier B.V. All rights reserved.
http://dx.doi.org/10.1016/j.mee.2012.07.046

on the basis of thermionic emission diffusion (TED) theory reveals an abnormal decrease of the barrier height (BH) and increase of the ideality factor with decreasing temperature [22–24]. The temperature dependent characteristic parameters for Schottky barrier diodes can be succesfully explained on the basis of TE mechanism with Gaussian distribution of the barrier heights.

Gallium arsenide is one of the most popular semiconductors that has intrinsic electrical properties superior to silicon, such as a direct energy gap, higher electron mobility, a high breakdown voltage, chemical inertness, mechanical stability, and lower power dissipation [25,26]. These advantages of gallium arsenide are attractive to experimentally investigate the influence of illumination intensity and temperature on the electrical characteristics of Al/p-GaAs/In structure.

The manuscript is on the electrical characteristics of Al/p-GaAs contacts. We aim to experimentally investigate the electrical properties of Al/p-GaAs structure under illumination and temperature conditions. In present work, we reported the experimental results of *I–V* and *C-V* characteristics of this particular structure as a function of illumination and temperature.

2. Experimental details

The substrate used in this study is p-GaAs (100)-doped zinc (Zn). p-GaAs wafer was sequentially cleaned with trichloroethylene, acetone and methanol. Then, the wafer was rinsed in de-ionized water of 18 M Ω-cm and was dried with high purity N_2. The native oxide on the surface was etched in sequence with acid solutions (H_2SO_4:H_2O_2:H_2O = 3:1:1) for 60 s, and (HCl:H_2O = 1:1) for another 60 s. Again, the wafer was rinsed in de-ionized water and was dried with N_2. An ohmic contact on back contact to p-type GaAs wafer was formed by vacuum thermal evaporation of Al metal and was thermally treated at 370 °C for 5 min in N_2 atmosphere. Then, the above procedures were also used to clean the front surface. Finally, circular dots with a diameter of approximately 2 mm of Au were then evaporated through a molybdenum mask at a pressure of $2x10^{-5}$mbar to form the Schottky barriers. Thus, Al/p-GaAs Schottky diodes were obtained. Before the Al evaporating, the surface morphology and roughness of GaAs substrate were investigated using Park System XE-100E atomic force microscopy (AFM). Fig. 1 shows AFM images of the GaAs substrate surface. The scan size of the image is 10×10 μm^2. The surface roughness for GaAs was found to be 11.686 nm. It means that the substrate surface was perfectly smooth. High flatness of the substrate surface causes high quality metal/semiconductor interface. The current–voltage (*I–V)* and capacitance–voltage (*C-V*) measurements of the device were made using a 4200 SCS semiconductor characterization system. Illumination measurements were employed under the light intensities of 20–150 mW/cm^2 using a light source consisting of 500 W halogen lamp. The intensity of the light was measured by solar power meter (Model TM-206).

3. Results and discussion

3.1. Illumination intensity dependence of the I–V characteristics

The current (I) through a SBD at a forward bias (V), according to thermionic emission (TE) theory, is given by the following relation [1,2]

$$I = I_o \exp\left(\frac{q(V - IR_s)}{nkT}\right) \quad (1)$$

where, I_0 is the reverse saturation current given by

$$I_0 = AA^*T^2 \exp\left(-\frac{q\Phi_b}{kT}\right) \quad (2)$$

where q is the electronic charge, V is the definite forward-bias voltage, A^* is the effective Richardson constant, A is the diode contact area, k is the Boltzmann constant, T is the absolute temperature, Φ_b is the barrier height and n is the ideality factor. Fig. 2 shows the forward and reverse bias *I–V* characteristics of the Al/p-GaAs diode under dark and various illumination intensities at room temperature. The current at a given voltage for Al/p-GaAs diode under illumination is higher than that of the current under dark. The forward current at high bias region is increased with the increasing illumination intensity due to the fact that photons can generate electron–hole pairs in the depletion layer of the semiconductor. This indicates that the light illumination increases the production of electron–hole pairs. The increase in charge production is dependent on the difference in the electron affinities between metal and semiconductor. When the device is illuminated, electrons in the valence band of the GaAs absorb energy, and they are able to jump to the conduction band [27].

The values of Φ_b and n were determined from the intercept and the slopes of the forward bias $ln(I)$vs. voltage (V) plot, respectively. The values of I_0 obtained by extrapolating the linear intermediate bias-voltage region of the ln*I–V* curve to zero applied bias-voltage and the barrier height (BH) values calculated from Eq. (2) were shown in Table 1. As shown in Table 1, the BH and n values were found to be a strong function of illumination intensity. The values of BH were found to increase, while the values of n are decreased with the increasing illumination level (BH = 0.642 eV and n = 1.38 under 20 mW/cm^2 and BH = 0.644 eV and n = 1.27 under 40 mW/cm^2). The illumination dependence of the BH can be described as

$$\Phi_{b0}(P) = \Phi_{b0} - \alpha P \quad (3)$$

where α is the illumination coefficient of GaAs band gap and P is the intensity of illumination. The fitting of $\Phi_{b0}(P)$ yields $\Phi_{b0} = 0.639$ eV and $\alpha = -1.03 \times 10^{-4}$ eV/W. This value of illumination coefficient of the BH is in agreement with the temperature coefficient of the GaAs band gap (-8.50×10^{-4} eV/K). Similar results have been reported with α values of 2×10^{-4} eV/K [1]. This result indicates that the electrical characteristics of SBDs vary with illumination and this device can be used as an optical sensor for optoelectronic applications. Al/p-GaAs diode exhibits a good rectifying behavior with a relatively low leakage current density. There are several effects, which cause deviations of the ideal behavior and must be taken into account. These effects can be interface states and series resistance and these are important parameters for the diode performance. These parameters cause a downward curvature in *I–V* characteristics at higher forward bias values. The value of R_s is decreased with the increasing illumination intensity due to the charge being excited from the valance band to conductance band; therefore this case creates the downward curvature in the forward bias *I–V* plots under illumination to shift towards high bias region as shown in Fig. 2. This effect causes to the non-linear region of the forward bias ln*I–V* curves of the diode. In such a case, Cheung's method can be used to obtain the barrier height, ideality factor and series resistance. Cheung's functions are expressed by the following relations [28]

$$\frac{dV}{d(\ln I)} = \frac{nkT}{q} + IR_s \quad (4)$$

$$H(I) = V - \left(\frac{nkT}{q}\right)\ln\left(\frac{I}{AA^*T^2}\right) \quad (5)$$

$$H(I) = n\Phi_{b0} + IR_s \quad (6)$$

Eq. (4) should give a straight line for the data in the downward curvature region of the forward bias *I–V* characteristics. Fig. 3

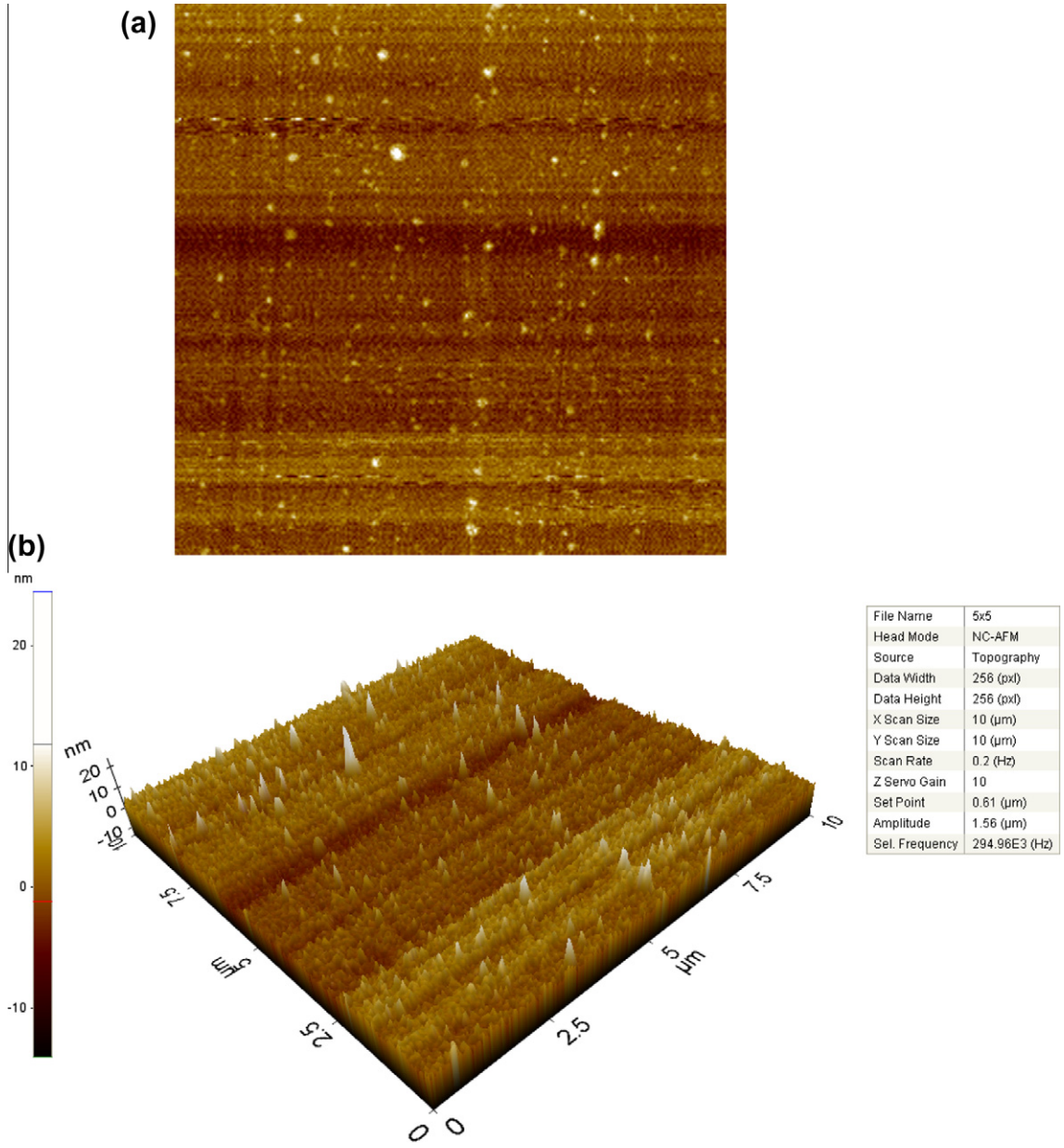

Fig. 1. AFM images of the native GaAs substrate surface (a) one-dimensional (1D), (b) three-dimensional (3D).

shows the experimental dV/dln(I) vs. I and H(I) vs. I plots of the Al/p-GaAs SBD in dark and under different illumination intensities at room temperature. Thus, the values of n and R_s were obtained from the intercept and slope of the dV/dln(I) vs. I plots (Fig. 3a) at each illumination level, respectively. The plots of H(I) vs. I (Fig. 3b) give a straight line with a current axis intercept equal to $n\,\Phi_{b0}$. The slopes of these plots also provide a second determination of R_s, which can be used to check the consistency of this approach. As function of illumination intensity, the values of R_s obtained from Eq. (4) are given in Table 1. It is possible to see similar evaluations in the literature [17,18,29–31]. The values of R_s were determined for a wide illumination range of 20–120 mW/cm^2. The R_s values of the diode were of order of 10^2 Ω. The results indicate a certain reduction in carrier density in the depletion region of the rectifier through the introduction of traps and recombination centers associated with illumination effect [32,33].

3.2. Illumination intensity dependence of the C–V characteristics

Fig. 4 shows that the photocapacitance dependence on the reverse bias has the form of a narrow peak located, where the barrier capacitance drops steeply with V_{rev}. The capacitance values vary from the strong inversion region (−3.0 V) to the strong accumulation region (+3.0 V). These changes in capacitance occur especially in the depletion and accumulation regions, while the values of capacitance remain almost constant decreasing in the inversion region. This makes it possible to determine the barrier capacitance C_I under extrinsic illumination and, hence, the photocapacitance,

$$C_{ph} = C_I - C_{dark} \tag{7}$$

With the increase of the illumination intensity, the concentration of charge carriers increases logarithmically. The increase of the charge carrier concentration under illumination leads to an improvement of the space charge layer [34]. The observed increase

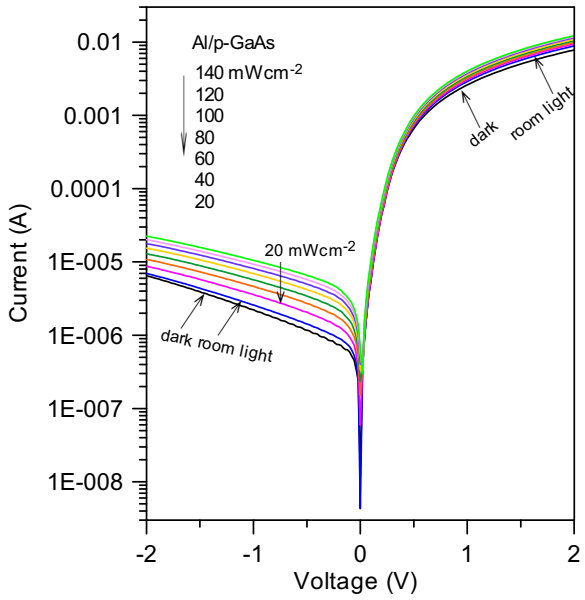

Fig. 2. The forward and reverse bias semi-logarithmic *I–V* characteristics of Al/p-GaAs diode in dark and under various illumination intensities at room temperature.

of capacitance with illumination may be qualitatively explained by the equivalent circuit model developed by Goswami and Goswami (G–G) [35] model of bulk resistance R_s in series with parallel *R–C*. According to this model, the measured capacitance *C* is given by [35]:

$$C = C_\infty + \frac{1}{w^2 R^2 C_\infty}, \tag{8}$$

where *R* is the resistance of the structure, $\omega = 2\pi f$ is the angular frequency, C_∞ is the capacitance at the higher frequency and *f* is the applied frequency. According to the above equation, the increase of capacitance *C* with illumination may be due to the decrease of the value of *R* with illumination, as shown in Table 1. The decrease in series resistance with increasing illumination is due to the increase of the free carriers with the effect of illumination. Accordingly, this can be explained by the enhancement of the photoconductivity of the Al/p-GaAs structure. It is clear from Eq. (8) that the decrease of *R* under the effect of illumination leads to the increase of the capacitance *C*. According to a method presented by Nicollian and Brews [36], the real series resistance of the MS structures can be calculated from the capacitance (*C*) and conductance (*G*) in strong accumulation region at sufficiently high frequencies [36] as

$$R_s = \frac{G}{G^2 + (wC)^2} \tag{9}$$

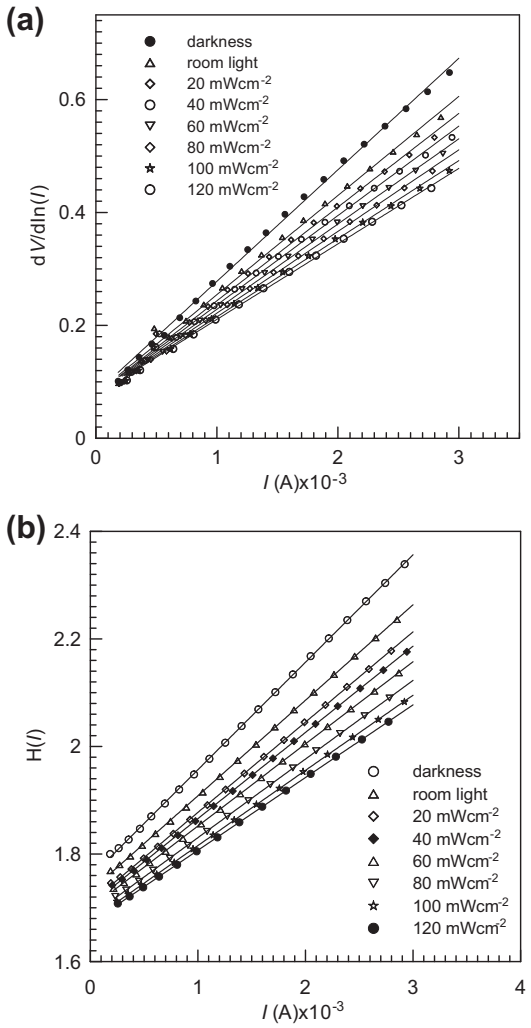

Fig. 3. (a) Experimental d*V*/dln(*I*) vs. *I* and (b) H(*I*) vs. *I* plots of Al/p-GaAs diode in dark and under various illumination intensities at room temperature.

It can be seen in Fig. 5, the values of R_s in the depletion and accumulation regions are increased with the increasing illumination intensity. This behavior can be attributed to the effect of the trap charges have enough energy to escape from the traps located at metal/semiconductor interface due to illumination effect.

3.3. Temperature dependence of the I–V characteristics

In order to obtain further insights into the carrier transport mechanism through the Al/p-GaAs contact, the *I–V* measurements were performed at different temperatures in the range of

Table 1
Illumination and temperature dependence of various parameters determined from forward bias *I–V* characteristics of Al/p-GaAs SBD.

Power (mW/cm^2)	Φ_b (eV) (eff.light)	*n* (eff.light)	I_0 (eff.light)	R_s (ohm)	Temp. (K)	Φ_b (eV) (eff.temp)	*n* Temp.	I_0 (Temp.)	R_s Temp.	N_{ss} (eV^{-1}/cm^2) (Temp.)
Dark	0.638	1.51	3.6971×10^{-7}	197	298	0.639	1.51	3.5671×10^{-7}	197	1.4871×10^{12}
Room L.	0.640	1.45	3.3571×10^{-7}	175	313	0.673	1.42	3.6671×10^{-7}	161	1.4671×10^{12}
20	0.642	1.38	3.1171×10^{-7}	165	333	0.712	1.31	4.8271×10^{-7}	144	1.4571×10^{12}
40	0.644	1.27	2.9671×10^{-7}	158	353	0.749	1.21	6.4771×10^{-7}	131	1.4471×10^{12}
60	0.647	1.14	2.6171×10^{-7}	150	373	0.787	1.14	8.4171×10^{-7}	117	1.4371×10^{12}
80	0.647	1.10	2.5671×10^{-6}	144	393	0.820	1.08	1.2171×10^{-6}	105	1.4171×10^{12}
100	0.648	1.07	2.4671×10^{-6}	138	413	0.853	1.05	1.7071×10^{-6}	93	1.4071×10^{12}
120	0.648	1.06	2.71×10^{-6}	133	423	0.870	1.02	1.9871×10^{-6}	89	1.3971×10^{12}

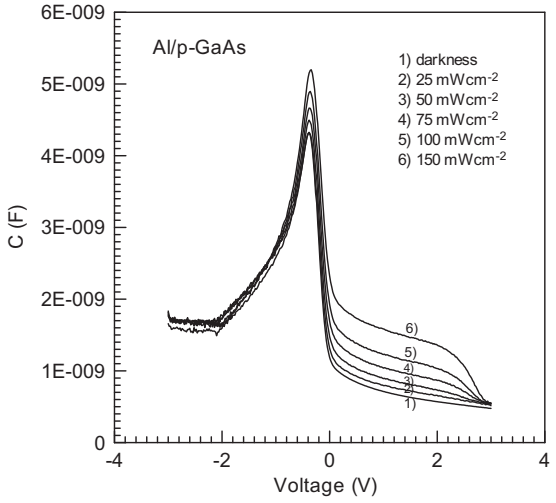

Fig. 4. Measured capacitance *C* vs. *V* plots of Al/p-GaAs diode in dark and under various illumination intensities.

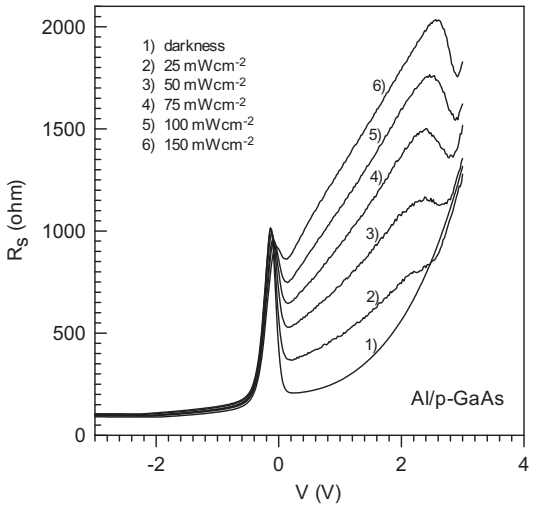

Fig. 5. The series resistance profile of Al/p-GaAs diode calculated from measured capacitance *C* data in dark and under various illumination intensities.

298–423 K. Fig. 6 shows the semi-logarithmic plot of the *I–V* curves of the Al/p-GaAs/In diode at various temperatures. From the current (*I*) through a SBD at a forward bias (*V*), according to thermionic emission (TE) theory, BH and *n* were obtained as in Table 1. The main diode parameters, *n* and zero-bias barrier height (apparent barrier height) (Φ_{b0}) were found to be strongly temperature dependent and while Φ_{b0} is decreased, the value of *n* is increased with decreasing temperature. Experimental d*V*/dln(*I*) vs. *I* and H(*I*) vs. *I* plots of Al/p-GaAs diode at different temperatures were shown in Fig. 7a and b. The values of R_s were determined for a temperature range of 298–423 K. The increase of R_s with decreasing temperature can be attributed to the reduction of free carrier concentration at low temperatures [22]. Since current transport across the metal–semiconductor interface is controlled by temperature, electrons at low temperature pass over the lower barriers and therefore current will flow through patches of the lower SBH and results in a larger ideality factor.

A spatial distribution of the barrier height at the MS interface of Schottky contacts by a Gaussian distribution has been suggested by Werner and Güttler [23,37] as:

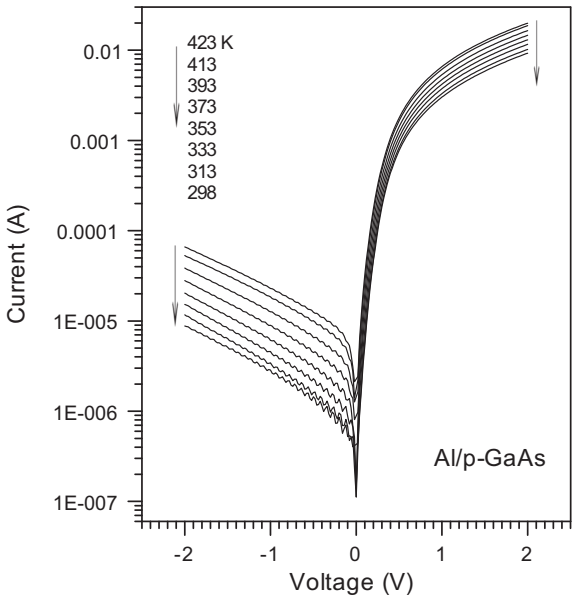

Fig. 6. Semi-logarithmic plots of both forward and reverse current vs. applied voltage at different temperatures.

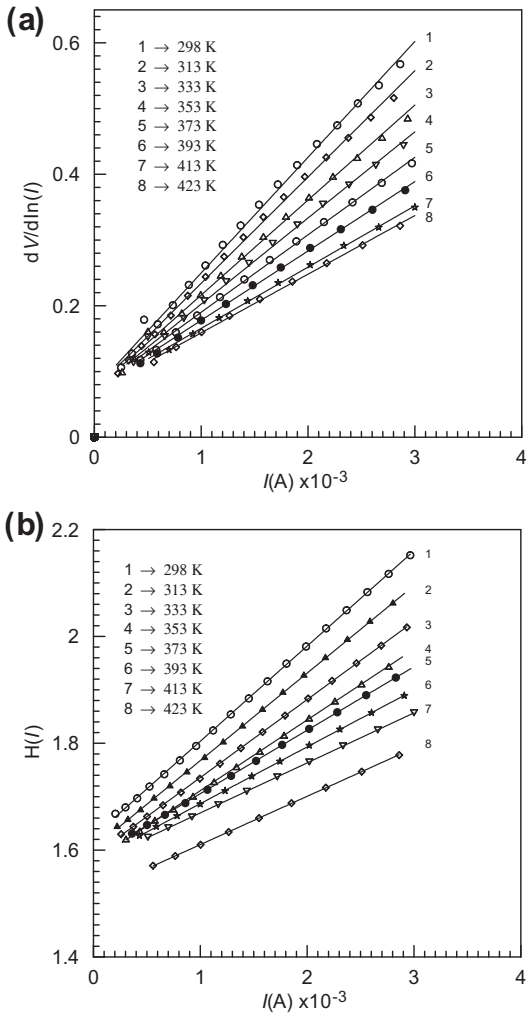

Fig. 7. (a) Experimental d*V*/dln(*I*) vs. *I* and (b) H(*I*) vs. *I* plots of Al/p-GaAs diode at different temperatures.

$$P(\Phi_b^j) = \frac{1}{\sigma_s\sqrt{2\pi}} \exp\left[-\frac{\left(\Phi_b^j - \bar{\Phi}_b^j\right)^2}{2\sigma_s^2}\right] \quad (10)$$

where $1/\sigma_s\sqrt{2\pi}$ corresponds to the normalization constant. The total current density through the Schottky contact is given by

$$J(V) = A^*T^2 \times \exp\left[-\frac{q}{kT}\left(\bar{\Phi}_b^j - \frac{q\sigma_s^2}{2kT}\right)\right]\exp\left(\frac{qV_d}{kT}\right)\left[1-\exp\left(-\frac{qV_d}{kT}\right)\right] \quad (11)$$

Since the BH is known to depend on the electric field and hence on the applied voltage, the entire profile is also affected by the bias. By assuming a linear bias dependence of both the mean barrier height ($\bar{\Phi}_b^j$) and square of the standard deviation (σ_s^2) with coefficients ρ_2 and ρ_3, (i.e., $\bar{\Phi}_b^j(V) = \bar{\Phi}_{b0}^j + \rho_2 V$ and $\sigma_s^2(V) = \sigma_{s0}^2 + \rho_3 V$), respectively, Eq. (11) gets modified as:

$$J = J_0 \exp\left(\frac{qV_d}{n_{ap}kT}\right)\left[1-\exp\left(-\frac{qV_d}{kT}\right)\right] \quad (12)$$

With

$$J_0 = A^*T^2 \exp\left(-\frac{q\Phi_{ap}}{kT}\right) \quad (13)$$

where, Φ_{ap} and n_{ap} are called as apparent zero-bias barrier height and apparent ideality factor, respectively, and are given by the following relations [23]

$$\Phi_{ap} = \bar{\Phi}_{b0}^j - \frac{q\sigma_{s0}^2}{2kT} \quad (14)$$

$$1/n_{ap}(T) - 1 = -\rho_1(T) = -\rho_2 + \frac{q\rho_3}{2kT} \quad (15)$$

where ρ_1, ρ_2 and ρ_3 are the voltage coefficients and depict the voltage deformation of the barrier height distribution, while $\bar{\Phi}_{b0}^j$ and σ_{s0} values are the mean barrier height and its standard deviation at the zero-bias ($V = 0$), respectively. Since Φ_{ap} depends on the distribution parameters $\bar{\Phi}_{b0}^j$ and σ_{s0}, and temperature, the decrease of the apparent zero-bias BH is affected by the existence of the interface inhomogeneities and this effect is particularly significant at low temperatures. On the other hand, the abnormal increase in n_{ap} comes up mainly due to the bias coefficients (ρ_2 and ρ_3) of the mean barrier height and the standard deviation. Whilst ρ_2 gives a constant shift, ρ_3 causes its temperature dependent variation and gets into significance at low temperature.

As Eqs. (2) and (13) are of the same form, the fitting of the experimental J–V data to Eq. (11) gives Φ_{ap} and n_{ap}, which should obey Eqs. (14) and (15). Thus, the plot of Φ_{ap} vs. $q/2kT$ (Fig. 8) should be a straight line yielding $\bar{\Phi}_{b0}^j$ and σ_{s0} from the intercept and slope, respectively. The values of 1.412 eV and 0.2 eV for $\bar{\Phi}_{b0}^j$ and σ_{s0}, respectively were obtained from the least-square linear fitting of the data. When comparing $\bar{\Phi}_{b0}^j$ and σ_{s0} parameters, it is seen that the standard deviation is $\approx 14.16\%$ of the mean zero bias barrier height. This value confirms the barrier height inhomogeneities arose from interfacial properties.

Fig. 8 also shows the $(1/n_{ap} - 1)$ vs. $1/2kT$ plot. According to Eq. (15), this plot should be a straight line that gives the voltage coefficients ρ_2 and ρ_3 from the intercept and slope, respectively. The values of $\rho_2 = -0.737$ and $\rho_3 = -0.056$ eV were obtained from this plot. The linear behavior of $(1/n_{ap} - 1)$ vs. $1/2kT$ plot confirms that the ideality factor does indeed denote the voltage deformation of the Gaussian distribution of the BH. It is clear from the Eq. (15) that when ρ_3 becomes negative, it will be responsible for the increase in n_{ap} with a decrease in temperature. As ρ_2 becomes also negative, we can conclude that the BH and its standard deviation are decreased as bias is increased. These results reveal that a bias voltage obviously homogenizes the BH fluctuation. Since the conventional Richardson plot deviates from linearity at low temperatures due to the barrier inhomogeneity, it can be modified by combining Eqs. (13) and (14) as follows:

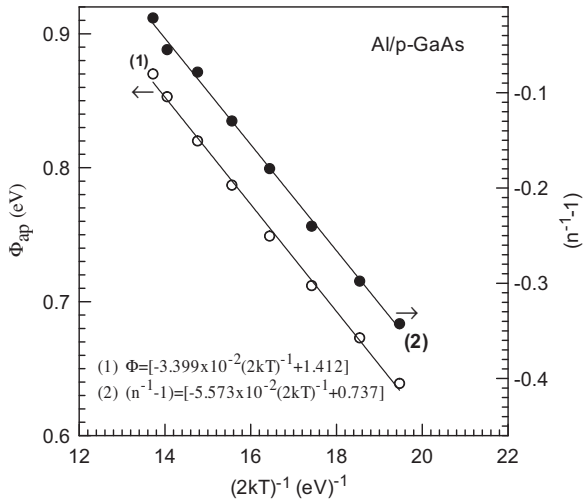

Fig. 8. Plots of Φ_{ap} -$1/2kT$ and $1/n_{ap}$-1 vs. $1/2kT$ of Al/p-GaAs diode.

$$In\left(\frac{J_0}{T^2}\right) - \left(\frac{q^2\sigma_{s0}^2}{2k^2T^2}\right) = InA^* - \frac{q\bar{\Phi}_{b0}^j}{kT} \quad (16)$$

Also, modified Richardson plot $[In(J_0/T^2) - (q^2\sigma_{s0}^2/2k^2T^2)$ vs. $1000/T]$ according to Eq. (16) should also be a straight line with the slope and the intercept at the ordinate directly yielding the zero-bias mean BH $\bar{\Phi}_{b0}^j$ and A^*, respectively. As seen in Fig. 9, the modified Richardson plot has a quite good linearity over the whole temperature range corresponding to single activation energy around $\bar{\Phi}_{b0}^j$. By the least-square linear fitting of the data, $\bar{\Phi}_{b0}^j$=1.417 eV and A^*=93.06 $AK^{-2}cm^{-2}$ were obtained. Meanwhile, this value of $\bar{\Phi}_{b0}^j = 1.417$ eV is approximately the same as the value of $\bar{\Phi}_{b0}^j = 1.412$ eV from the plot of Φ_{ap} vs. $1/2kT$ given in Fig. 8, while modified Richardson constant A^*=93.06 $AK^{-2}\,cm^{-2}$ is higher

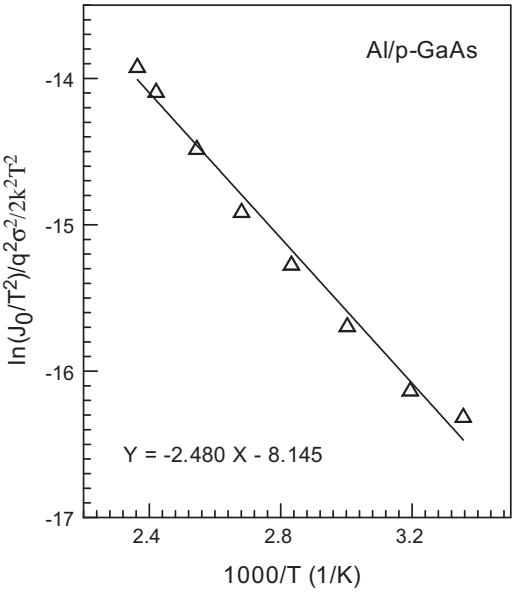

Fig. 9. Plot of $\ln(J_0/T^2)$-$q^2\,\sigma_s^2\,/2k^2T^2$ vs. $1000/T$ of Al/p-GaAs diode.

than that of the theoretical value of $A^* = 8.16\ AK^{-2}\ cm^{-2}$. These results show that the temperature dependent *I–V* characteristics of Al/p-GaAs Schottky structure obey the Gaussian distribution of BHs due to the BH inhomogeneities prevailing at the metal–semiconductor interface.

The effective barrier height (Φ_e) and n are assumed to be bias-dependent due to the presence of an interfacial layer and interface states located at the interfacial layer-semiconductor interface and defined as [38]

$$\Phi_e = \Phi_b + \left(\frac{d\Phi_e}{dV}\right)V = \Phi_b + \beta V \tag{17}$$

$$n = \frac{q}{kT}\left[\frac{V}{In(I/I_0)}\right] = 1 + \frac{\delta}{\varepsilon_i}\left[\frac{\varepsilon_s}{W_D} + qN_{ss}\right] \tag{18}$$

where β is the voltage coefficient of the effective barrier height. Φ_e is a parameter that includes the effects of both interface states in equilibrium with the semiconductor [38]. The interface state density (N_{ss}) is expressed by Card and Rhoderick [38] for MIS structure in equilibrium as;

$$N_{ss} = \frac{1}{q}\left[\frac{\varepsilon_i}{\delta}(n(V) - 1) - \frac{\varepsilon_s}{W_D}\right] \tag{19}$$

where δ the thickness of interfacial insulator layer, W_D is the width of the space charge region, ε_i and ε_s are the permittivity of the interfacial insulator layer and the semiconductor, respectively. Furthermore, in p-type semiconductors, the energy of interface states E_{ss} with respect to the top of the valance band, at the semiconductor surface, is given by [39]

$$E_{ss} - E_v = q(\Phi_e - V) \tag{20}$$

Thus, the energy distribution of the interface states in equilibrium with the semiconductor as a function of V may be determined by means of Eqs. (19) and (20) by taking into account the bias dependence of the ideality factor and BH. Fig. 10 shows the curves of interface state density distribution determined from the downward concave curvature region of the experimental semi-logarithmic forward bias *I-V* characteristics of the Al/p-GaAs diode. As seen in Fig. 10, the exponential growth of the interface state densities from midgap towards the top of the valance band is very apparent. The values of interface state density N_{ss} ($\approx 10^{12}$ $eV^{-1}\ cm^{-2}$) are reasonable for metal/GaAs SBDs [40,41]. The values of N_{ss} decrease with increasing illumination intensity between the (E_v – 0.35) and (E_v – 0.60) eV. It can be deduced that the carriers' excitations had decreased the trap effects at the interface [31]. The obtained results indicate that the illumination dependence of N_{ss} values of Al/p-GaAs structure are not different from that for N_{ss} values of Al–TiW–Pd_2Si/n-Si SBD [18] and are different from that for p-ZnTe/n-CdMnTe/GaAs magnetic diode [19]. The effect of illumination can be considered as a new source of increasing or decreasing interface density states. The decrease in N_{ss} value with the increasing illumination intensity may be explained by charge and discharge of interface states under illumination effect. Also, the chemical interaction and interfacial polarization at the interface of heterojunction diodes as at the oxide–inorganic interface states will give rise to new interface states. Furthermore, the values of N_{ss} are decreased with increasing temperature. This phenomenon is a result of molecular restructuring and reordering of the metal–semiconductor interface under the effect of temperature [42]. The interface states and interfacial layer between the metal/semiconductor structures play an important role in the determination of the characteristic parameters of the devices.

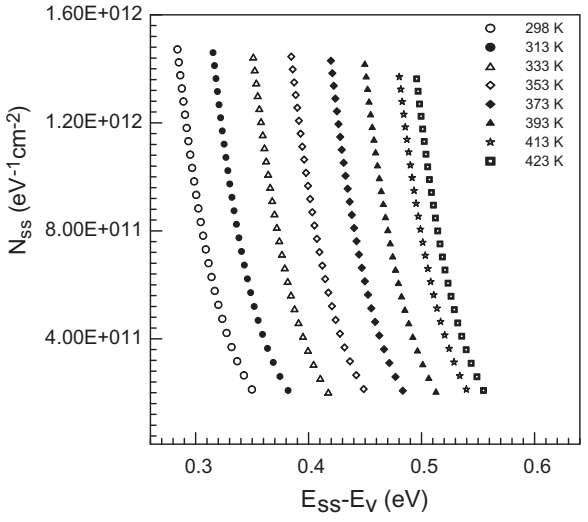

Fig. 10. The energy distribution profile of the N_{ss} obtained from the forward bias *I–V* characteristics of Al/p-GaAs diode in dark and at different temperatures.

4. Conclusions

The effects of illumination and temperature on electrical properties of Al/p-GaAs diode have been investigated under various illumination and temperature conditions. The reverse bias *I–V* characteristics of the diode under illumination exhibited a high photosensitivity. Experimental results show that the main electrical parameters such as the BH, n, R_s, and N_{ss} values were found to depend on the illumination intensity and temperature, strongly. The values of R_s have been obtained from Cheung's method. The capacitance and the resistance of the prepared device show illumination dependence. The increase of the capacitance with illumination is associated with an improvement of the space charge layer due to the transfer of photo-generated electrons and holes. But, the decrease of resistance with illumination is associated with the generation of charge carriers. The obtained results confirm that the Al/p-GaAs/In diode is a MS type photodiode and can be a candidate material in a light sensitive capacitor in modern electronic devices. The temperature-dependent data analysis revealed an increase in the zero bias barrier height and decrease in the ideality factor with increasing temperature. Abnormal behaviors in the temperature dependent ideality factor and the barrier height in the Al/p-GaAs diode have been interpreted accounting the TE theory with a Gaussian distribution of the BH having spatial variations. The interface state density distribution was determined from the experimental semi-logarithmic forward bias *I–V* characteristics by taking the bias dependence of the effective barrier height into account and found to decrease with the increasing illumination intensity.

Acknowledgments

This study is a result of the international collaboration program between teams at King Abdulaziz University, Saudi Arabia and Fırat University, Turkey.

References

[1] S.M. Sze, Physics of Semiconductor Device, 2nd edn., John Wiley & Sons, New York, 1981.
[2] E.H. Rhoderick, R.H. Williams, Metal-Semiconductor Contacts, 2nd edn., Clarendon Press, Oxford, 1988.
[3] A. Neamen Donald, Semiconductor Physics and Devices, Irwin, Boston, 1992.
[4] J. Singh, Semiconductor Devices, Basic Principles, John Wiley & Sons, New York, 2001.
[5] M.C. Petty, M. Bryce, An Introduction to Molecular Electronics, Oxford University Press, NewYork, 1995.

[6] C. Joachim, M.A. Ratner, Molecular Electronics, American Chemical Society, Washington D.C., 1997.
[7] T. Tanaka, M. Tanaka, M. Itakura, T. Sadoh, M. Miyao, Thin Solid Films 518 (2010) S170–S173.
[8] S. Hayashi, M. Nangu, T. Morikuni, S. Owa, N.S. Takahashi, J. Cryst. Growth 311 (2009) 842–846.
[9] J. Kobayashi, N. Ohashi, H. Sekiwa, I. Sakaguchi, M. Miyamoto, Y. Wada, Y. Adachi, K. Matsumoto, H. Haneda, J. Cryst. Growth 311 (2009) 4408–4413.
[10] S. Sommadossi, L. Litynska, P. Zieba, W. Gust, E.J. Mittemeijer, Mater. Chem. Phys. 81 (2003) 566–568.
[11] Z. Bao, A.J. Lovinger, A. Dodabalapur, Appl. Phys. Lett. 69 (1996) 3066.
[12] M. Ishii, Y. Taga, Appl. Phys. Lett. 80 (2002) 3430.
[13] C.W. Tang, Appl. Phys. Lett. 48 (1986) 183.
[14] P. Peumans, S.R. Forrest, Appl. Phys. Lett. 79 (2001) 126.
[15] S. Heutz, P. Sullivan, B.M. Sanderson, S.M. Schultes, T.S. Jones, Sol. Energy Mater. Sol. Cells 83 (2004) 229.
[16] P. Peumans, V. Bulovic, S.R. Forrest, Appl. Phys. Lett. 76 (2000) 3855.
[17] A.A.M. Farag, A. Ashery, E.M.A. Ahmed, M.A. Salem, J. Alloys Comp. 495 (2010) 116.
[18] H. Uslu, S. Altındal, U. Aydemir, I. Dokme, I.M. Afandiyeva, J. Alloys Comp. 503 (2010) 96.
[19] G.B. Sakr, I.S. Yahi, J. Alloys Comp. 503 (2010) 213.
[20] K.C. Kao, W. Hwang, Electrical Transport in Solids with Particular Reference to Organic Semiconductors, Pergamon Pres Ltd., Headington Hill Hall, Oxford, England, 1981.
[21] M.A. Lampert, P. Mark, Current Injection in Solids, Academic Press, New York, London, 1970.
[22] S. Chand, J. Kumar, J. Appl. Phys. 80 (1) (1996) 288.
[23] J.H. Werner, H.H. Güttler, J. Appl. Phys. 69 (3) (1991) 1522.
[24] C.T. Chuang, Solid State Electron. 27 (1984) 299.
[25] R.V. Ghita, C. Logofatu, C. Negrila, A.S. Manea, M. Cernea, M.F. Lazarescu, J. Optoelectronics Adv. Materials 7 (2005) 3033.
[26] M. Soylu, F. Yakuphanoglu, J. Alloys Compd. 506 (2010) 418.
[27] F. Yakuphanoglu, Solar Cells 91 (2007) 1182.
[28] S.K. Cheung, N.W. Cheung, Appl. Phys. Lett. 49 (1986) 85.
[29] A.A.M. Farag, I.S. Yahia, M. Fadel, Int. J. Hydrogen Energy 34 (2009) 4906.
[30] F. Yakuphanoglu, J. Alloys Compd. 494 (2010) 451.
[31] B. Akkal, Z. Benamara, N.B. Bouiadjra, S. Tizi, B. Gruzza, Appl. Surf. Sci. 253 (2006) 1065.
[32] M.Y. Feteha, M. Soliman, N.G. Gomaa, M. Ashry, Renew. Energy 26 (2002) 113.
[33] R.K. Hanna, K. Ip, K.K. Allums, K. Baik, C.R. Abernathy, S.J. Pearton, Y.W. Heo, D.P. Norton, F. Ren, S. Shojan-Ardalan, R. Wilkins, J. Electron. Mater. 34 (2005) 395.
[34] V. Dyakonov, D. Godovsky, J. Meyer, J. Parisi, C.J. Brabec, N.S. Sariciftci, J.C. Hummelen, Synth. Met. 124 (2001) 103.
[35] A. Goswami, A.P. Goswami, Thin Solid Films 16 (1973) 175.
[36] E.H. Nicollian, J.R. Brews, MOS Physics and Technology, Wiley, New York, 1982.
[37] J.H. Werner, H.H. Güttler, J. Appl. Phys. 73 (3) (1993) 1315.
[38] H.C. Card, E.H. Rhoderick, J. Phys. D: Appl. Phys. 4 (1971) 1589.
[39] P. Cova, A. Singh, A. Medina, R.A. Masut, Solid-State Electron. 42 (1998) 477.
[40] A.F. Ozdemir, A. Turut, A. Kokçe, Thin solid films (2003) 210–215.
[41] S. Karatas, A. Turut, Physica B 381 (2006) 199–203.
[42] B. Akkal, Z. Benamara, A. Boudissa, N.B. Bouiadjra, M. Amrani, L. Bideux, B. Gruzza, Mater. Sci. Eng. B 55 (1998) 162.